In-Situ Magnetic Susceptibility Measurements As a Tool to Follow Geomicrobiological Transformation of Fe Minerals

5 AUTHORS, INCLUDING:

Urs Dippon
Umweltbundesamt, Germany
10 PUBLICATIONS **178** CITATIONS

SEE PROFILE

Moti Lal Rijal
9 PUBLICATIONS **83** CITATIONS

SEE PROFILE

Erwin Appel
University of Tuebingen
175 PUBLICATIONS **2,551** CITATIONS

SEE PROFILE

Andreas Kappler
University of Tuebingen
215 PUBLICATIONS **4,886** CITATIONS

SEE PROFILE

In-Situ Magnetic Susceptibility Measurements As a Tool to Follow Geomicrobiological Transformation of Fe Minerals

KATHARINA PORSCH,[†,§] URS DIPPON,[†] MOTI LAL RIJAL,[‡,⊥] ERWIN APPEL,[‡] AND ANDREAS KAPPLER[†,*]

Geomicrobiology, Geophysics, Center for Applied Geosciences, University of Tuebingen, Sigwartstrasse 10, D-72076 Tuebingen, Germany

Fe minerals sorb nutrients and pollutants and participate in microbial and abiotic redox reactions. Formation and transformation of Fe minerals is typically followed by mineral analysis at different time points. However, in lab studies the available sample amount is often limited and sampling may even influence the experimental conditions. We therefore evaluated the suitability of in situ magnetic susceptibility (MS) measurements, which do not require sampling, as an alternative tool to follow ferro(i)magnetic mineral (trans-)formation during ferrihydrite reduction by *Shewanella oneidensis* MR-1, and in soil microcosms. In our experiments with MR-1, a large initial increase in volume specific MS (κ) followed by a slight decrease correlated well with the initial formation of magnetite and further reduction of magnetite to siderite as also identified by μ-XRD. The presence of humic acids retarded magnetite formation, and even inhibited magnetite formation completely, depending on their concentration. In soil microcosms, an increase in κ accompanied by increasing concentrations of HCl-extractable Fe occurred only in microbially active set-ups, indicating a microbially induced change in soil Fe mineralogy. Based on our results, we conclude that MS measurements are suitable to follow microbial Fe mineral transformation in pure cultures as well as in complex soil samples.

Introduction

Fe minerals are ubiquitous in the environment. Under anoxic and pH neutral conditions Fe(II) minerals such as Fe(II) carbonate (siderite), Fe(II) phosphate (vivianite), or mixed-valent Fe minerals (e.g., magnetite) are present. At neutral pH, Fe(III) exists mainly as Fe(III) (hydr)oxides and oxyhydroxides such as ferrihydrite (Fh), hematite and goethite (*1*).

* Corresponding author: Geomicrobiology, Center for Applied Geosciences, University of Tuebingen, Sigwartstrasse 10, D-72076 Tuebingen, Germany E-mail address: andreas.kappler@uni-tuebingen.de Telephone: +49-7071-2974992 Fax: +49-7071-295059.
† Geomicrobiology.
‡ Geophysics.
§ Current address: UFZ - Helmholtz Centre for Environmental Research, Department of Bioenergy, Permoserstraße 15, D-04318 Leipzig, Germany.
⊥ Current address: Hetauda Campus, Institute of Forestry, Tribhuvan University, Hetauda, Nepal.

Fe(II) can be oxidized abiotically by MnO_2, nitrite and molecular O_2 (*2–4*) or biotically by anaerobic phototrophic and nitrate-reducing, as well as aerobic Fe(II)-oxidizing microorganisms (*5, 6*). Reduction of Fe(III) minerals can occur under anoxic conditions abiotically by sulfide and reduced humic substances (*7, 8*) or biotically by Fe(III)-reducing microorganisms (*9*). The type of Fe minerals formed during Fe redox reactions depends on geochemical parameters such as pH, rate of Fe^{2+} supply, and presence of other ions (*10–12*).

Abiotic and microbial Fe mineral (trans)formation processes are intensively studied due to their environmental relevance. For example, under Fe(III)-reducing conditions, the degradation of organic contaminants is directly coupled to microbial Fe(III) reduction (*13*). Furthermore, Fe minerals affect the mobility of nutrients and toxic compounds. Arsenic, for example, coprecipitates during Fe(III) mineral formation (*14*) and gets released when these minerals are dissolved (*15*).

Experimental studies aiming to understand the biogeochemical processes involved in Fe mineral (trans)formation face several problems. First, to follow Fe mineral (trans)formation over time, e.g. by X-ray diffraction, spectroscopy or by sequential Fe extraction, it is necessary to sample at different time points, which might disturb the experimental system due to shaking during the sampling procedure. Second, sampling removes significant amounts of the sample volume which may influence further mineral (trans-)formation. This is particularly relevant for Fe mineral identification by sophisticated techniques such as X-ray diffraction, Mössbauer spectroscopy, or X-ray absorption spectroscopy that require significant sample amounts (*16*). Third, in many cases, access to these techniques is limited and the measurements, including sample preparation and data analysis, are time-consuming. Fourth, the content of a formed Fe mineral might be under the detection limit for some of these techniques, especially when complex samples (e.g., soils, sediments) with a high content of other minerals (e.g., clay minerals, quartz) are studied. Therefore, it would be helpful to have an analytical technique that can follow Fe mineral (trans)formation and identify formed Fe minerals, even in small amounts, without sampling and large technical effort.

Magnetic susceptibility (MS) measurements might be such an alternative for systems in which ferro(i)magnetic Fe minerals are (trans)formed. MS describes how strongly a substance is magnetized in an external magnetic field. Diamagnetic materials (e.g., quartz, water) have a small, negative MS. Paramagnetic minerals (e.g., siderite, ferrihydrite) and antiferromagnetic minerals with spin-canting (hematite) or defect moments (goethite) have a small, positive MS, whereas ferromagnetic elements (e.g., metallic Fe) and ferrimagnetic minerals have a very high (e.g., magnetite, maghemite, greigite), or moderately high (e.g., pyrrhotite), positive MS (*17*). For simplicity the term ferro(i)magnetic minerals is used in this study and it refers to ferrimagnetic minerals and antiferromagnetic minerals with spin-canting or defect moments. Although MS of a sample is a bulk signal of all compounds, ferro(i)magnetic minerals dominate the MS or, if their concentration is very low, also paramagnetic Fe phases may be important. However, MS of a sample does not only depend on the concentration but also on the size (more precisely: magnetic domain state) and shape of these minerals (*18*).

Analysis of magnetic properties of dried minerals formed by microbial Fe(III) reduction has been used before to quantify the amount of magnetite formed (*19, 20*). Hence,

this method might be also applicable for in situ measurements in cultures of Fe-metabolizing microorganisms or in soil microcosms. The aim of this study was to evaluate whether in situ MS measurements can be used (i) to monitor ferro(i)magnetic mineral formation in pure cultures of Fe(III)-reducing microorganisms, (ii) to determine how humic acids influence ferro(i)magnetic mineral formation in these cultures, and (iii) to follow Fe mineral (trans)formation in soils by MS measurements.

Materials and Methods

Ferrihydrite, humic acids. Fh was synthesized according to (21), washed four times with MilliPore water, deoxygenated by repeated evacuation and N_2-flushing, and autoclaved. Pahokee peat humic acids (PPHA) were purchased from the International Humic Substances Society. For a stock solution, 5 mg/mL PPHA were dissolved in 88.6 mM NaCl solution and the pH adjusted to 7.0 with NaOH. The solution was filtered (0.22 μm, mixed cellulose ester) into sterile anoxic (100% N_2) glass bottles.

Bacteria and Growth Media. *Shewanella oneidensis* MR-1 was kept as frozen stock at −80 °C. Cells streaked out on Luria−Bertani (LB) agar plates were incubated oxically for 24 h at 28 °C and stored for up to 10 days at 4 °C. One colony was transferred into 10 mL anoxic freshwater medium containing 20 mM Na-lactate and 40 mM fumarate. After 72 h at 28 °C, 200 μL of this culture were transferred to 10 mL fresh anoxic freshwater medium and incubated for 48 h at 28 °C. LB agar contained per L 10 g tryptone, 5 g yeast extract, 5 g NaCl and 12 g agar. Freshwater medium was prepared as described in ref 22. LML medium modified from that in ref 23 contained per L 0.2 g yeast extract, 0.1 g peptone and 20 mM Na-lactate. Freshwater and LML medium were prepared anoxically, buffered at pH 7.0−7.1 with 30 mM $NaHCO_3$, and used with a headspace of $N_2:CO_2$ (90:10).

Experimental Set-up with MR-1. Experiments with MR-1 were performed in 60 mL serum bottles containing 25 mL LML medium, 15 mM Fh and 2×10^5 cells/mL. Bottles containing PPHA (final concentration of 210 and 630 mg/L) were equilibrated for 48 h prior to inoculation. The cultures were incubated at 28 °C in the dark.

Experimental Set-up with Soil. Top soil (∼20 cm) from the Schoenbuch forest (Sbu) and Fraeulinsberg (Fb), both southwest Germany, was sampled. Selected soil properties are given in Supporting Information (SI) Table S1. Microcosms consisted of 21 g of soil Sbu in 60 mL serum bottles. For sterile set-ups, the soil was autoclaved twice with 2 days of incubation at room temperature in between. Two different set-ups were prepared: addition of (i) 10 mL water, no additional carbon source, and (ii) 10 mL of a lactate/acetate solution (15 mM each). The headspace was flushed with $N_2:CO_2$ (90:10). The microcosms were incubated at 28 °C in the dark and mixed once per week.

Analytical Techniques. *Fe extraction.* For Fe quantification in MR-1 cultures, 100 μL of culture suspension was extracted in 900 μL of 0.5 M HCl for 2 h at room temperature. After centrifugation (15 min, 20 817g), Fe(II) and total Fe (Fe_{tot}) were quantified by the ferrozine assay (24) as described in ref 22. Fe from soil Sbu was extracted before incubation (original soil without amendment) and after incubation. Prior to extraction, the microcosm bottles were centrifuged (10 min, 2000 rpm) and the supernatant was stored in 15 mL sterile plastic cups at −28 °C for dissolved organic and inorganic carbon (DOC, DIC) analysis (see below). Fe extractions from three subsamples of the original soil Sbu and three subsamples of the soil pellets collected after incubation were performed after (25, 26) with a soil:extractant ratio (w/v) of 1:50. The first subsample was extracted with Na-acetate (pH 5) for 24 h and the second subsample with 0.5 M HCl for 1 h, both at room temperature on a shaker. The

third subsample was extracted with 1 M HCl at 70 °C in a water bath for 24 h and the extracts were cooled for 15 min at room temperature. From all extracts, 1.8 mL was centrifuged (15 min, 20,817 g) to remove soil particles. Fe(II) and Fe_{tot} in the supernatants were quantified by the ferrozine assay. In the Na-acetate extracts only Fe_{tot} was quantified.

MS Measurements. Low-field MS of the experimental bottles was measured with a KLY-3 Kappabridge (AGICO, Czech Republic) at room temperature with a peak magnetic field intensity of 300 A/m and a frequency of 875 Hz. The medium and soil in the bottles were entirely placed within the homogeneity range of the pick-up coil. Each bottle was measured three times and the values were averaged. Results in this study are given in volume specific MS (κ) for a reference volume of 10 cm^3. Values of κ are only relative as the effective sample volume cannot be determined. This, however, does not affect the significance of MS results for measurements performed on the same sample over time. In the case of liquid cultures, κ of each bottle measured directly after setting up the experiment was subtracted from all following κ values in order to correct for the bottle, stopper, and medium.

Quantification of Dissolved PPHA. Since the LML medium had a high organic carbon background concentration, dissolved PPHA could not be quantified by DOC analysis in MR-1 cultures. Therefore, 2 mL of sample was centrifuged (2 min, 20 817g) and the absorbance of the supernatant was measured at 465 nm in polystyrene microtiterplates with a microplate reader (FlashScan 550, Analytik Jena, Germany). A calibration curve was obtained in the range of 0−500 mg PPHA/L with a quantification limit of 10 mg PPHA/L.

μ-XRD. Fe minerals were identified by μ-X-ray diffraction (μ-XRD) (Bruker D8 Discover XRD instrument, Bruker AXS, Germany). The minerals from one serum bottle were successively centrifuged (2 min, 9700g) into a 2 mL plastic cup, washed twice with anoxic water, and dried at room temperature in an anoxic glovebox (100% N_2). Dried minerals were ground in an agate mortar, resuspended in anoxic ethanol, and transferred to a silicon wafer that was covered with a polyethylene foil to prevent oxidation of the minerals during measurements under oxic conditions.

Dissolved Carbon Measurements. The supernatant sampled from the soil microcosms was thawed, centrifuged (10 min, 5000g) and filtered (0.22 μm, mixed cellulose esters). The DOC and DIC contents were determined with a carbon analyzer (high TOC, Elementar, Germany).

Results and Discussion

Magnetic Mineral Formation by *Shewanella oneidensis* MR-1. In order to determine if MS measurements can be used to follow ferro(i)magnetic mineral formation in pure cultures of Fe(III)-reducing microorganisms, reduction of 15 mM Fh by *S. oneidensis* MR-1, an Fe(III)-reducer known to be able to produce magnetite during Fh reduction, was followed over time by Fe(II) quantification, MS measurements and μ-XRD mineral analysis. The amount of extractable Fe(II) increased strongly during the first 5 days, followed by a slower increase to a value of $66.0 \pm 0.9\%$ Fe(II):Fe_{tot} at day 18 (Figure 1A), demonstrating Fh reduction by MR-1. During incubation with MR-1, the orange-brown color of the Fh turned dark brown to black (SI Figure S1) and in contrast to Fh, these minerals did not dissolve completely in 0.5 M HCl, indicating that transformation of Fh to another less soluble Fe-phase took place. The volume specific MS (κ) increased strongly to 7803 ± 26 μSI between days 2 and 5 (Figure 1B), indicating the formation of a ferro(i)magnetic mineral phase. The maximum κ of 7910 ± 173 μSI was measured after 7 days. The following slow decrease until day 18 to 6896 ± 170 μSI suggested that the formed magnetic mineral was probably further reduced by MR-1 and transformed into another Fe(II)-phase. This is supported by the accompanying slow increase
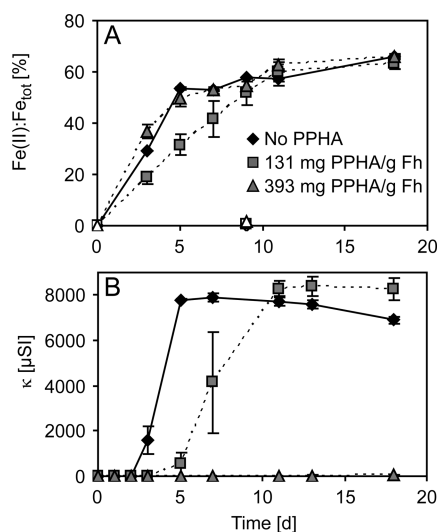
FIGURE 1. Reduction of 15 mM ferrihydrite (Fh) by *Shewanella oneidensis* MR-1. (A) Changes in the Fe(II):Fe$_{tot}$ ratio determined by 0.5 M HCl extraction and (B) changes in volume specific magnetic susceptibility (κ) in absence of PPHA ($\blacklozenge$), in presence of 131 mg PPHA/g Fh (all PPHA sorbed, gray solid square), and in presence of 393 mg PPHA/g Fh (PPHA sorbed and in solution, gray solid triangle). Open symbols in (A) represent sterile controls. Results are means of duplicates. Bars bracket the range of duplicates.

FIGURE 2. μ-XRD patterns of minerals formed during reduction of 15 mM ferrihydrite (Fh) by *Shewanella oneidensis* MR-1. (A) Minerals formed in absence of PPHA after 4, 8, and 20 days of incubation. (B) Minerals formed after 20 days of incubation in presence of 131 mg PPHA/g Fh (all PPHA sorbed) and 393 mg PPHA/g Fh (PPHA sorbed and in solution). Reference lines represent magnetite (solid lines) and siderite (dashed lines). The gray bar indicates the range where signals appear from the foil used to cover the samples to prevent oxidation by oxygen.

in Fe(II) concentration and siderite formation (see below). However, it has to be noted that the decrease in κ might also be caused by an increase of grain size; if part of the magnetite particles grow above the critical volume of the superparamagnetic to single domain transition, the overall κ value of the sample could decrease because of the lower κ of single domain particles compared to the smaller superparamagnetic grains.

In abiotic controls, neither the formation of Fe(II) (Figure 1A) nor an increase in κ was observed (data not shown). Control experiments with MR-1 cultures subjected seven times to MS measurements in comparison to cultures which were subjected only twice to MS measurements revealed that MS measurements did not influence Fh reduction by MR-1 and hence are noninvasive for the microorganisms (SI Figure S2).

Fe(II) and κ data of bottles that were set up in parallel for μ-XRD analysis were similar to the data shown in Figure 1 (data not shown). For μ-XRD mineral analysis, bottles were sacrificed either after 4 days (during the strong increase in κ), 8 days (approximately maximum κ) or 20 days (after the slight decrease of κ) of incubation, respectively. μ-XRD measurements revealed that at day 4 and 8 only magnetite was present as crystalline Fe mineral phase, whereas at day 20, siderite was also detected (Figure 2A). Depending on the Fe(III) reduction rate and the presence of other ions, microbial Fh reduction can also lead to the formation of other Fe minerals such as goethite and hematite (10). However, besides magnetite and siderite we did not detect any other Fe minerals by μ-XRD measurements (Figure 2A). Hence, the initial increase in κ was due to the formation of magnetite (a ferrimagnetic Fe(II)−Fe(III)-mineral with a high κ). Magnetite formation during microbial amorphous Fe(III) mineral reduction was first shown by Lovley et al. (27). Analysis of magnetic properties of magnetite formed by the Fe(III)-reducing bacterium *Geobacter metallireducens* revealed that the magnetite particles covered a broad grain size distribution (28). Since the κ value of ferro(i)magnetic minerals depends on their size and shape (17), analysis of the content of these minerals in microbial cultures using MS
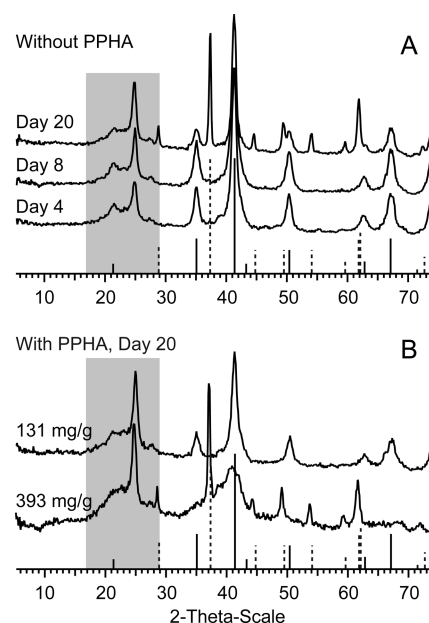
data is only semiquantitatively possible (see example for such a calculation in the SI S1, Figure S3). In order to determine the exact amount of magnetite formed, further analyses using different methods such as measurements of the saturation magnetization are necessary, as illustrated in SI S1.

The detection of siderite (a paramagnetic mineral with a low κ) by XRD at the end of the experiment (Figure 2A) confirmed that part of the formed magnetite was further reduced, as indicated by the decrease of κ at day 18. This is in line with previous research showing reduction of magnetite by *S. oneidensis* MR-1 (29, 30). Microbial formation of magnetite and siderite in bicarbonate buffered medium was also observed by Fredrickson and co-workers (12) during reduction of 45 mM hydrous ferric oxide by *Shewanella putrefaciens* CN32. However, since the authors identified the minerals only after 20 days of incubation, they could not determine if magnetite was first produced and then further reduced to siderite or if siderite was an initial reaction product. In a follow up study Dong et al. (29) showed that *S. putrefaciens* CN32 can indeed reduce biogenic magnetite to some extent and that siderite is formed during this reduction in bicarbonate buffered medium. However, Zachara et al. (10) also performed reduction experiments with Fh (20 mM) and *S. putrefaciens* CN32 and observed that depending on the N$_2$:CO$_2$ ratio either only magnetite (up to 95:5 N$_2$:CO$_2$), a mix of Fe minerals (90:10), or only siderite (80:20) was formed. They concluded that siderite is not formed via magnetite, but that high bicarbonate concentrations prevent Fe(II) adsorption on Fh, a process that is necessary for Fh conversion into magnetite. In contrast, our κ values and μ-XRD data indicated that magnetite was formed at the beginning of the Fh reduction and was then further reduced to siderite. Overall, this experiment showed that MS measurements are suitable to follow microbial magnetite (trans)formation in pure cultures of *S. oneidensis* MR-1 and, in combination with other techniques (e.g., measurements

of the saturation magnetization), can give insights into Fe mineral (trans)formation pathways on even a quantitative basis.

Influence of PPHA on Microbial Magnetite Formation. In order to follow ferro(i)magnetic mineral formation by MS measurements in more complex systems such as soils, geochemical factors influencing magnetite formation need to be evaluated. Humic substances are ubiquitous in the environment. They influence microbial Fe(III) reduction and Fe mineral transformation by complexation of Fe(II) and Fe(III), by facilitating electron transfer from the cells to Fe(III) minerals (electron shuttling), and by sorption to Fe minerals (31–34). We therefore determined the influence of PPHA on Fh reduction and magnetite formation by *S. oneidensis* MR-1. Two concentrations of PPHA were chosen in order to have one set-up where the PPHA were virtually completely sorbed to the Fh (131 mg PPHA/g Fh) and one where a significant fraction of the PPHA remained in solution (393 mg PPHA/g Fh with 152 ± 34 mg dissolved PPHA/g Fh). The two PPHA concentrations were selected based on a sorption isotherm of PPHA to Fh (SI Figure S4).

The extent of Fh reduction after 18 days of incubation was similar in set-ups without PPHA addition, with all PPHA sorbed, and with PPHA sorbed but also present in solution (ratio of Fe(II):Fe$_{tot}$ of $63.4 \pm 2.2\%$ to $66.0 \pm 0.9\%$, Figure 1A). However, in the set-up with only sorbed PPHA, the Fh reduction rate was slower than in the absence of PPHA, whereas in the system containing both sorbed and dissolved PPHA, the Fh reduction rate was similar to that without PPHA. In set-ups with only sorbed PPHA (131 mg PPHA/g Fh), a black mineral was formed within 25 days (SI Figure S1). The supernatant in set-ups containing 393 mg PPHA/g Fh was initially dark brown due to the presence of dissolved PPHA. During Fh reduction, the medium in these set-ups turned light brownish indicating significant removal of PPHA from solution and after 25 days of incubation a black mineral was formed.

Although the extent of Fh reduction (Figure 1A) and the color of the formed minerals were similar independent of the added PPHA concentration (SI Figure S1), MS measurements revealed significant mineralogical differences between the different set-ups. In the case of only sorbed PPHA, the κ value started to increase 2 days later and the increase was slower than in the absence of PPHA (Figure 1B). The maximum κ of 8373 ± 439 μSI measured after 13 days was only slightly higher than in set-ups without PPHA, indicating that a similar amount of magnetite was formed in both set-ups. However, in contrast to the set-ups without PPHA, no significant decrease in κ occurred after the maximum κ was reached. In set-ups where both sorbed and dissolved PPHA were present, κ increased by only 34 ± 4 μSI over 18 days, indicating that no ferro(i)magnetic mineral (i.e., no magnetite) was formed. μ-XRD analysis of minerals formed in parallel set-ups supported the κ data. In set-ups containing only sorbed PPHA, only magnetite and no siderite was present after 20 days of incubation confirming the κ values that remained stable after the initial increase and indicating that no further reduction of magnetite occurred within the incubation time. Since the experiments were terminated after 18 days, the set-ups containing only sorbed PPHA were incubated for only another 5 days after reaching the maximum κ, in contrast to 11 days for set-ups without PPHA (Figure 1B). Thus, a potential further transformation of the magnetite into siderite in the presence of only sorbed PPHA after a longer incubation cannot be ruled out. When both sorbed and dissolved PPHA were present, only siderite was identified as a crystalline Fe mineral phase, which supports the small increase in κ. The dark color of the minerals in these set-ups was probably due to sorption of the PPHA to the siderite, which is usually white in color.

In our experiments, the addition of PPHA affected the Fh reduction rate, but not the extent of reduction (Figure 1A). It is known that the addition of humic and fulvic acids can increase Fe reduction rate by electron shuttling (31, 33, 35). Jiang and Kappler (35) determined that a minimum amount of ~10 mg/L dissolved PPHA must be present to stimulate Fh reduction by *S. oneidensis* MR-1, whereas Wolf et al. (36) showed that already 1 mg/L of groundwater aquifer humic acids was sufficient to stimulate Fh reduction by *Geobacter metallireducens*. In our experiments with 131 mg PPHA/g Fh, the amount of dissolved PPHA was <0.5 mg/L and therefore no electron shuttling and stimulation of Fh reduction was expected. The sorption of PPHA to Fh even had a negative effect on the reduction rate. In set-ups where a significant amount of PPHA was initially present in solution (152 ± 34 mg dissolved PPHA/g Fh = 236 ± 66 mg dissolved PPHA/L), the inhibitory effect of the sorbed PPHA was overcome and the reduction rate was as high as without PPHA added (Figure 1A). This suggests that *S. oneidensis* MR-1 used the dissolved PPHA to at least some extent as electron shuttle. However, despite the high concentration of initially dissolved PPHA, no stimulation of Fh reduction occurred in comparison to set-ups without PPHA. This is probably due to the fact that the initially dissolved PPHA were to a large extent removed from solution during Fh reduction as indicated by the color change of the solution from dark to light brown (SI Figure S1). This indicates that less electron shuttling molecules were available and therefore the stimulating effect of dissolved PPHA was reduced.

As indicated by both μ-XRD and MS analysis, the two different concentrations of PPHA had different effects on secondary mineral formation. In set-ups with only sorbed PPHA the Fe(II):Fe$_{tot}$ ratio on the day at which the κ value started to increase was approximately $29.2 \pm 0.0\%$. A similar Fe(II):Fe$_{tot}$ ratio ($31.6 \pm 4.1\%$) was found in set-ups without PPHA when the increase in κ started. These Fe(II):Fe$_{tot}$ ratios are comparable to that of stoichiometric magnetite (Fe(II):Fe$_{tot}$ = 33%) suggesting that a threshold Fe(II):Fe$_{tot}$ ratio of around 30% must be reached to initiate magnetite formation. Since Fh reduction in set-ups with only sorbed PPHA was slower than in PPHA-free set-ups, the Fe(II):Fe$_{tot}$ threshold ratio was reached later, leading to a later start of magnetite formation and a slower magnetite formation rate (Figure 1B). In the case where both sorbed PPHA and dissolved PPHA were present, no magnetite formation occurred at all, suggesting that the humic acids completely inhibited magnetite formation from Fh. Magnetite forms from Fh either via dissolution-reprecipitation or solid state conversion. For both pathways, adsorption of Fe(II) to Fh is necessary (37, 38). In contrast to the experiments without PPHA and with only sorbed PPHA (where part of the Fh was not covered by PPHA and therefore available for the conversion into magnetite), all sorption sites were obviously blocked when PPHA were present in excess, and therefore no transformation of the remaining Fh into magnetite was possible.

Fe mineral Transformation in Soil Monitored by MS Measurements. After the experiments with pure cultures of *S. oneidensis* MR-1 demonstrated that MS measurements are suitable to follow microbial Fe(III) mineral transformation, in particular magnetite formation and transformation, we determined whether this technique can also be used to monitor changes in the ferro(i)magnetic Fe mineralogy of soils. To this end, microcosm experiments with soil Sbu were set up either without the addition of organic carbon or with the addition of lactate/acetate. Lactate and acetate are easily degradable by microorganisms and were added to determine if Fe mineral (trans)formation in the soil Sbu was limited by the bioavailable organic carbon content.
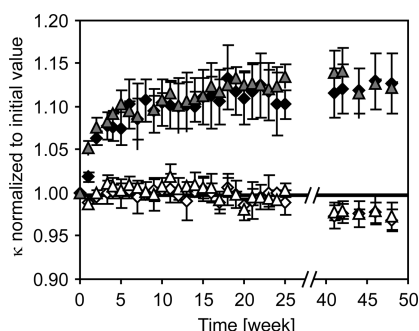
FIGURE 3. Changes in volume specific magnetic susceptibility (κ) over time of microbially active soil microcosms amended with 10 mL of water (♦) and 10 mL of 15 mM lactate/acetate solution (gray solid triangle). Open symbols represent sterile microcosms. The κ values measured at each time point were normalized by the κ value measured directly after setting up the microcosms. Solid horizontal line indicates κ without any change over time. Results are means of four replicates. Bars indicate the standard deviation.

FIGURE 4. (A) Fe extracted with Na-acetate (pH 5, room temperature), 0.5 M HCl (room temperature) and 1 M HCl (70 °C) from pellets obtained after centrifugation of sterile and microbially active soil microcosms amended with 10 mL of water (no C added) and 10 mL of 15 mM lactate/acetate solution. Open bars represent Fe(II), filled bars Fe$_{tot}$. Results are means of triplicate measurements of one bottle per set-up. Bars indicate the standard deviation. (B) Dissolved inorganic (DIC) and organic carbon (DOC) in the supernatants taken from the same bottles as in (A) after centrifugation. Results are means of duplicates. Bars bracket the range of duplicates.

The κ value of sterile microcosms did not change considerably over time (Figure 3). In contrast, the κ value of the microbially active microcosms increased significantly within the first 5−6 weeks followed by a slower increase until week 20 when the increase in κ leveled off. The extent of κ increase was not statistically different between microbially active set-ups either with or without organic carbon amendment, that is, $12.2 \pm 2.9\%$ for microcosms without carbon addition and $12.9 \pm 1.6\%$ for microcosms with lactate/acetate (calculated by averaging the last five κ measurements). Before the microcosms were set up, different Fe fractions were extracted from the field wet soil Sbu with Na-acetate (Fe$_{tot}$: 1.1 ± 0.1 μmol/g wet weight (ww)), 0.5 M HCl (Fe$_{tot}$: 27.9 ± 1.4 μmol/g ww, Fe(II): 4.0 ± 0.1 μmol/g ww) and 1 M HCl at 70 °C (Fe$_{tot}$: 231.3 ± 1.0 μmol/g ww, Fe(II): 161.3 ± 4.3 μmol/g ww). After approximately one year the microcosms were opened and the different Fe fractions of the incubated soil were determined. For each extracted fraction, the Fe$_{tot}$ and Fe(II) contents of the sterile microcosms were similar to the content of the original soil Sbu (Figure 4A), indicating that autoclaving, as well as incubation for approximately one year at 28 °C did not change the soil Fe redox speciation and mineralogy significantly. The Fe$_{tot}$ extracted with 1 M HCl at 70 °C was similar in both sterile and microbial active microcosms showing that the total Fe content was similar in all bottles. However, with the weaker extractants (Na-acetate and 0.5 M HCl) that quantify sorbed and poorly crystalline (bioavailable) Fe, more Fe$_{tot}$ was extracted from soil Sbu of microbially active set-ups than from sterile ones. Furthermore, the Fe(II):Fe$_{tot}$ ratio of the Fe fractions extracted with 0.5 M HCl and 1 M HCl at 70 °C was much larger in the microbially active set-ups than in the sterile ones. Both MS measurements and Fe extraction data showed that (i) the changes in κ were due to a change in the Fe mineralogy of the soil and (ii) that these changes were microbially driven. Since in the microbially active set-ups the κ values increased over time, the concentration of ferro(i)magnetic Fe minerals in the soil Sbu must have increased. The most important ferro(i)magnetic minerals in soils are magnetite (Fe$_3$O$_4$) and maghemite (γ-Fe$_2$O$_3$) (18) and one or both of these minerals might have been formed in the microbially active microcosms. In order to determine the sensitivity of our method, in an additional experiment soil from Fraeulinsberg (SI Table S1) was mixed with varying amounts of synthetic magnetite and κ was determined. We found that an increase in the amount of Fe present in the form of magnetite relative to the total amount of Fe in the soil by only 1 wt.%, increased the soil κ value by about 55% (not shown). The κ of the
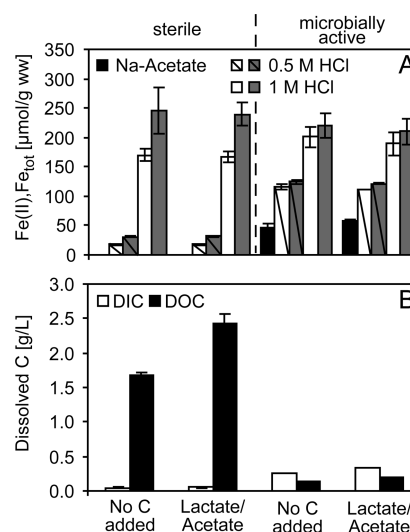
microbially active microcosms changed by only ∼10% (Figure 3), showing that MS measurements are a very sensitive tool able to detect even very small changes in the ferro(i)magnetic mineral content of soils.

Changes in κ and Fe speciation/mineralogy were similar in microbially active set-ups without organic carbon addition and with lactate/acetate addition, suggesting that organic carbon was bioavailable even without addition of lactate/acetate. Dissolved organic matter represents the most bioavailable organic carbon source in soils (39) and was probably leached from soil Sbu in the microcosms by the added water. In order to evaluate this hypothesis, we quantified DOC and DIC in the soil microcosms. In sterile microcosms amended with lactate/acetate, the DOC was 0.8 g/L higher than in sterile microcosms without carbon addition (Figure 4B). Lactate/acetate were both added at a concentration of 15 mM yielding a theoretical DOC of 0.9 g/L, thus 89% of the added carbon was recovered in the soil−water after one year (the rest was probably sorbed to soil particles such as Fe minerals (40)). In both organic carbon amended and nonamended microbially active set-ups the DOC was lower than 0.2 g/L, indicating efficient consumption of the bioavailable organic carbon by the microorganisms. Organic carbon mineralization was also evidenced by the DIC present in nonsterile compared to sterile set-ups. The DIC in the water of both the sterile set-ups was 0.05 ± 0.01 g/L, whereas in the microbially active set-ups it was much higher, varying between 0.25 ± 0.01 and 0.33 ± 0.00 g/L (Figure 4B).

The DOC, DIC, and κ values suggest that even without lactate/acetate addition, a large amount of bioavailable organic carbon was present. Although more DOC was initially present in set-ups with added lactate/acetate, this did not lead to more Fe mineral (trans)formation, indicating that either the bioavailable amount of Fe was limiting, or that the addition of lactate/acetate also stimulated microorganisms which were not involved in Fe redox reactions.

Application and Environmental Significance of in Situ MS Measurements. Fh reduction experiments with *S. oneiden-*

sis MR-1 showed that in contrast to wet-chemical Fe extraction data, in situ MS measurements were able to precisely detect the beginning of magnetite (trans)formation. Since MS measurements are fast, do not influence microbial activity, and can be done in situ and therefore do not require sampling, a high time resolution can be obtained. This allows the identification of sampling points for more detailed analyses that require more analytical effort (e.g., sequential Fe extraction, XRD, synchrotron-based analysis). The combination of MS measurements with these techniques can help to determine biogeochemical conditions for ferro(i)magnetic mineral (trans)formation and to identify the minerals present at different time points. Furthermore, the influence of environmentally relevant factors (e.g., humic substances) on ferro(i)magnetic mineral (trans)formation can easily be determined.

MS measurements over time of soil microcosms revealed that changes in κ can be used to follow microbial Fe mineral transformation processes even in complex environmental systems. The results showed that microbial Fe mineral transformation is accompanied by a consumption of bio-available organic carbon. The mobilization of organic carbon by water as observed in our soil microcosms is unlikely to happen in the environment in well drained soils as well as in organic carbon poor soils. However, the input of organic carbon to these soils, for example, in form of hydrocarbons or other organic contaminants, might induce a similar microbially driven change in the ferro(i)magnetic soil mineral content to that caused by the mobilization of organic carbon. Field studies in hydrocarbon-contaminated soils and areas with natural oil reservoirs have indeed shown differences in the soil mineralogy compared to uncontaminated areas, including differences in the ferro(i)magnetic mineral content (for a review see ref *41*). Since surface MS measurements in the field can be performed quickly and easily, large areas can be screened with a high spatial resolution. We therefore believe that MS measurements can serve as a fast and inexpensive tool to localize hydrocarbon contaminated areas in the field.

Acknowledgments

Supporting Information Available

Soil properties and the methods for their determination (Table S1), images of *S. oneidensis* MR-1 culture bottles over time (Figure S1), influence of MS measurements on Fh reduction by MR-1 (Figure S2), a description of the quantification of magnetite formed during Fh reduction by MR-1 (S1), temperature dependent MS measurement of magnetite (Figure S3) and sorption of PPHA to Fh (Figure S4). This material is available free of charge via the Internet at http://pubs.acs.org.

Literature Cited

(1) Cornell, R. M.; Schwertmann, U. *The Iron Oxides, Structure, Properties, Reactions, Occurences and Uses*; Wiley-VCH: Weinheim, 2003.

(2) Myers, C. R.; Nealson, K. H. Microbial reduction of manganese oxides - interactions with iron and sulfur. *Geochim. Cosmochim. Acta* **1988**, *52* (11), 2727–2732.

(3) Moraghan, J. T.; Buresh, R. J. Chemical reduction of nitrite and nitrous-oxide by ferrous iron. *Soil Sci. Soc. Am. J.* **1977**, *41* (1), 47–50.

(4) Stumm, W.; Lee, G. F. Oxygenation of ferrous iron. *Ind. Eng. Chem.* **1961**, *53* (2), 143–146.

(5) Emerson, D. Microbial oxidation of Fe(II) and Mn(II) at circumneutral pH. In *Environmental Microbe-Metal Interactions*; Lovley, D. R., Ed.; ASM Press: Washington, D.C., 2000.

(6) Kappler, A.; Straub, K. L. Geomicrobiological cycling of iron. *Rev. Mineral. Geochem.* **2005**, *59*, 85–108.

(7) Afonso, M. D.; Stumm, W. Reductive dissolution of iron(III) (hydr)oxides by hydrogen sulfide. *Langmuir* **1992**, *8* (6), 1671–1675.

(8) Bauer, I.; Kappler, A. Rates and extent of reduction of Fe(III) compounds and O_2 by humic substances. *Environ. Sci. Technol.* **2009**, *43* (13), 4902–4908.

(9) Lovley, D. R. Dissimilatory Fe(III) and Mn(IV) reduction. *Microbiol. Rev.* **1991**, *55* (2), 259–287.

(10) Zachara, J. M.; Kukkadapu, R. K.; Fredrickson, J. K.; Gorby, Y. A.; Smith, S. C. Biomineralization of poorly crystalline Fe(III) oxides by dissimilatory metal reducing bacteria (DMRB). *Geomicrobiol. J.* **2002**, *19*, 179–207.

(11) Hansel, C. M.; Benner, S. G.; Fendorf, S. Competing Fe(II)-induced mineralization pathways of ferrihydrite. *Environ. Sci. Technol.* **2005**, *39* (18), 7147–7153.

(12) Fredrickson, J. K.; Zachara, J. M.; Kennedy, D. W.; Dong, H.; Onstott, T. C.; Hinman, N. W.; Li, S.-M. Biogenic iron mineralization accompanying the dissimilatory reduction of hydrous ferric oxide by a groundwater bacterium. *Geochim. Cosmochim. Acta* **1998**, *62* (19/20), 3239–3257.

(13) Lovley, D. R.; Anderson, R. T. Influence of dissimilatory metal reduction on fate of organic and metal contaminants in the subsurface. *Hydrogeol. J.* **2000**, *8*, 77–88.

(14) Hohmann, C.; Winkler, E.; Morin, G.; Kappler, A. Anaerobic Fe(II)-oxidizing bacteria show As resistance and immobilize As during Fe(III) mineral precipitation. *Environ. Sci. Technol.* **2010**, *44* (1), 94–101.

(15) Islam, F. S.; Gault, A. G.; Boothman, C.; Polya, D. A.; Charnock, J. M.; Chatterjee, D.; Lloyd, J. R. Role of metal-reducing bacteria in arsenic release from Bengal delta sediments. *Nature* **2004**, *430* (6995), 68–71.

(16) Geesey, G. G.; Neal, A. L.; Suci, P. A.; Peyton, B. M. A review of spectroscopic methods for characterizing microbial transformations of minerals. *J. Microbiol. Methods* **2002**, *51* (2), 125–139.

(17) Dunlop, D. J.; Özdemir, Ö. *Rock Magnetism: Fundamentals and Frontiers*; Cambridge University Press: Cambridge, 1997.

(18) Mullins, C. E. Magnetic susceptibility of soil and its significance in soil science—A review. *J. Soil Sci.* **1977**, *28* (2), 223–246.

(19) Salas, E. C.; Berelson, W. M.; Hammond, D. E.; Kampf, A. R.; Nealson, K. H. The impact of bacterial strain on the products of dissimilatory iron reduction. *Geochim. Cosmochim. Acta* **2010**, *74* (2), 574–583.

(20) Behrends, T.; Van Cappellen, P. Transformation of hematite into magnetite during dissimilatory iron reduction—Conditions and mechanisms. *Geomicrobiol. J.* **2007**, *24* (5), 403–416.

(21) Raven, K. P.; Jain, A.; Loeppert, R. H. Arsenite and arsenate adsorption on ferrihydrite: Kinetics, equilibrium, and adsorption envelopes. *Environ. Sci. Technol.* **1998**, *32* (3), 344–349.

(22) Hegler, F.; Posth, N. R.; Jiang, J.; Kappler, A. Physiology of phototrophic iron(II)-oxidizing bacteria: implications for modern and ancient environments. *FEMS Microbiol. Ecol.* **2008**, *66* (2), 250–260.

(23) Myers, C. R.; Myers, J. M. Ferric iron reduction-linked growth yields of *Shewanella putrefaciens* MR-1. *J. Appl. Bacteriol.* **1994**, *76* (3), 253–258.

(24) Stookey, L. L. Ferrozine - a new spectrophotometric reagent for iron. *Anal. Chem.* **1970**, *42* (7), 779–781.

(25) Moeslund, L.; Thamdrup, B.; Jørgensen, B. B. Sulfur and iron cycling in a coastal sediment: Radiotracer studies and seasonal dynamics. *Biogeochemistry* **1994**, *27*, 129–152.

(26) Roden, E. E.; Zachara, J. M. Microbial reduction of crystalline iron(III) oxides: Influence of oxide surface area and potential for cell growth. *Environ. Sci. Technol.* **1996**, *30*, 1618–1628.

(27) Lovley, D. R.; Stolz, J. F.; Jr Nord, G. L.; Phillips, E. J. P. Anaerobic production of magnetite by a dissimilatory iron-reducing microorganism. *Nature* **1987**, *330* (6145), 252–254.

(28) Moskowitz, B. M.; Frankel, R. B.; Bazylinski, D. A.; Jannasch, H. W.; Lovley, D. R. A comparison of magnetite particles produced anaerobically by magnetotactic and dissimilatory iron-reducing bacteria. *Geophys. Res. Lett.* **1989**, *16* (7), 665–668.

(29) Dong, H.; Fredrickson, J. K.; Kennedy, D. W.; Zachara, J. M.; Kukkadapu, R. K.; Onstott, T. C. Mineral transformation associated with the microbial reduction of magnetite. *Chem. Geol.* **2000**, *169*, 299–318.

(30) Kostka, J. E.; Nealson, K. H. Dissolution and reduction of magnetite by Bacteria. *Environ. Sci. Technol.* **1995**, *29*, 2535–2540.

(31) Lovley, D. R.; Coates, J. D.; Blunt-Harris, E. L.; Phillips, E. J. P.; Woodward, J. C. Humic substances as electron acceptors for microbial respiration. *Nature* **1996**, *382* (6590), 445–448.

(32) Lovley, D. R.; Blunt-Harris, E. L. Role of humic-bound iron as an electron transfer agent in dissimilatory Fe(III) reduction. *Appl. Environ. Microbiol.* **1999**, *65* (9), 4252–4254.

(33) Royer, R. A.; Burgos, W. D.; Fisher, A. S.; Jeon, B. H.; Unz, R. F.; Dempsey, B. A. Enhancement of hematite bioreduction by natural organic matter. *Environ. Sci. Technol.* **2002**, *36* (13), 2897–2904.

(34) Kaiser, K.; Mikutta, R.; Guggenberger, G. Increased stability of organic matter sorbed to ferrihydrite and goethite on aging. *Soil Sci. Soc. Am. J.* **2007**, *71* (3), 711–719.

(35) Jiang, J.; Kappler, A. Kinetics of microbial and chemical reduction of humic substances: implications for electron shuttling. *Environ. Sci. Technol.* **2008**, *42* (10), 3563–3569.

(36) Wolf, M.; Kappler, A.; Jiang, J.; Meckenstock, R. U. Effects of humic substances and quinones at low concentrations on ferrihydrite reduction by *Geobacter metallireducens. Environ. Sci. Technol.* **2009**, *43* (15), 5679–5685.

(37) Tronc, E.; Belleville, P.; Jolivet, J. P.; Livage, J. Transformation of ferric hydroxide into spinel by Fe(II) adsorption. *Langmuir* **1992**, *8* (1), 313–319.

(38) Jolivet, J. P.; Belleville, P.; Tronc, E.; Livage, J. Influence of Fe(II) on the formation of the spinel iron-oxide in alkaline medium. *Clays Clay Miner.* **1992**, *40* (5), 531–539.

(39) Marschner, B.; Kalbitz, K. Controls of bioavailability and biodegradability of dissolved organic matter in soils. *Geoderma* **2003**, *113* (3−4), 211–235.

(40) Filius, J. D.; Hiemstra, T.; Van Riemsdijk, W. H. Adsorption of small weak organic acids on goethite: Modeling of mechanisms. *J. Colloid Interface Sci.* **1997**, *195* (2), 368–380.

(41) Schumacher, D. Hydrocarbon-induced alteration of soils and sediments. In *Hydrocarbon Migration and Its Near-Surface Expression*; Schumacher, D., Abrams, M. A., Eds.; American Association of Petroleum Geologists: Tulsa, OK, 1996.